Jusami
Homepage: http://jusami.batan.go.id
Jurnal Sains Materi Indonesia
Akreditation No : 21/E/KPT/2018
Date 9 July 2018
ISSN 1411-1098
E-ISSN 2614-087X

TUNABLE SURFACE PLASMON RESONANCE OF Au@TiO_2 CORE-SHELL NANOPARTICLES ON THE DSSC PERFORMANCE

Friska Ayu Fitrianti Sugiono and Doty Dewi Risanti
Faculty of Industrial Technology, Institut Teknologi Sepuluh Nopember
Kampus ITS Keputih, Sukolilo, Surabaya, 6011, Indonesia
E-mail: friskaayuf@gmail.com

Received: 5 Desember 2018 *Revised: 5 March 2019* *Accepted: 19 March 2019*

ABSTRACT

TUNABLE SURFACE PLASMON RESONANCE OF Au@TiO_2 CORE-SHELL NANOPARTICLES ON THE DSSC PERFORMANCE. Plasmonic core-shell nanoparticles, i.e. gold can improve the efficiency of Dye-sensitized Solar Cell by increase the light harvesting due to the strong near-field effect LSPR (Localized Surface Plasmon Resonance). To achieve maximum enhancement, the morphology of core-shell need to be optimized with coated either by insulator such as semiconductor, i.e. TiO_2. In this paper, morphology of Au@TiO_2 core-shell precisely control by various TiO_2 volume and systematically study its influence on the plasmonic enhancement effect. A gold solution was prepared using Turkevich method. The crystal structure of the powders was determined by powder X-Ray Diffraction (XRD). The optical properties were measured by UV-Vis absorption spectroscopy using UV-Vis Lambda 750. The photocurrent action spectra or IPCE in visible light spectrum was obtained by adjusting wavelength of incident light, i.e. series connection of halogen lamp and monochromator. UV-Vis absorption spectra of core–shell showed the position of the surface plasmon Au band in the range of 500–550 nm. According to UV-Vis characterization, all samples studied show weak surface plasmon resonance response (~520 to 550 nm) as indicative of the thick TiO_2 shells for individual core-shell Au@TiO_2.

Keywords: DSSC, Photoanode, Core-shell structure, Plasmonic effecr, TiO_2

ABSTRAK

RESONENSI PLASMON PERMUKAAN TUNABLE Au @ TiO_2 CORE-SHELL NANOPARTIKEL TENTANG KINERJA DSSC. Nanopartikel inti-sel plasmonik, yaitu kaleng emas meningkatkan efisiensi Sel Surya Peka-sensitif dengan meningkatkan panen cahaya karena medan dekat yang kuat efek LSPR (Resonansi Plasmon Permukaan Lokal). Untuk mencapai peningkatan maksimum, morfologi core-shell perlu dioptimalkan dengan dilapisi baik oleh isolator seperti semikonduktor, yaitu TiO_2. Dalam makalah ini, morfologi Au-TiO_2 core-shell secara tepat mengontrol berbagai volume TiO_2 dan secara sistematis mempelajari pengaruh pada efek peningkatan plasmonik. Solusi emas disiapkan menggunakan metode Turkevich. Struktur kristal serbuk tersebut ditentukan oleh serbuk difraksi sinar-X (XRD). Sifat optik diukur dengan spektroskopi serapan UV-Vis menggunakan UV-Vis Lambda 750. Tindakan photocurrent spektra atau IPCE dalam spektrum cahaya tampak diperoleh dengan menyesuaikan panjang gelombang cahaya insiden, yaitu seri lampu halogen dan monokromator. Spektrum serapan UV-Vis dari core-shell menunjukkan posisi dari band plasmon Au permukaan di kisaran 500-550 nm. Menurut karakterisasi UV-Vis, semua sampel yang diteliti menunjukkan respons resonansi plasmon permukaan yang lemah (~ 520 hingga 550 nm) sebagai indikasi kerang TiO_2 yang tebal. untuk masing-masing core-shell Au @ TiO_2.

***Kata kunci*:** DSSC, Photoanode, Struktur Core-shell, Efek Plasmonic, TiO_2

INTRODUCTION

To improve the efficiency of Dye Sensitized Solar Cells (DSSC), there are several ways that can be done. One of them is by adding metal in a core-shell structure to increase the light harvesting due to the strong near-field effect LSPR [1,2]. There are metals commonly used for promoting LSPR in the visible region, i.e. gold (Au) [1,2], silver (Ag) [3], copper (Cu) [4] and bismuth (Bi) [5], among which Au is the most excellent metal exhibiting strong LSPR effect. The noble metal should be coated either by semiconductor i.e TiO_2. These shells provide resistance to degradation in the presence of the iodide/triiodide (I^-/I^{3-}) corrosive liquid electrolyte[3]. One may expect two beneficial mechanisms that may be involved in the efficiency enhancement for using TiO_2 semiconductor as shell. First, the hot electrons generated inside the resonant plasmonic cores can contribute directly to the photocurrent. Second, the metal cores can undergo charge equilibrium with the surrounding semiconductor and modify the Fermi level of TiO_2, resulting in an improved cell potential [4]. Therefore, the morphology of the core as well as the material used and the thickness of the shell need to be carefully designed and controlled in order to obtain optimal enhancement. In this paper, morphology of Au@TiO_2 core-shell precisely control by various TiO_2 volume and systematically study its influence on the plasmonic enhancement effect.

EXPERIMENTAL METHOD

Materials and Instruments

Materials used in this research consist of Titanium (III) chloride ($TiCl_3$, 15%), ethanol (absolute EtOH, Merck), ammonium (NH3, 25%), hydrochloric acid (HCl, 37%), sodium hydroxide (NaOH 28%, Merck), aquades, $HAuCl_4 \cdot 3H_2O$ (49%, Sigma Aldrich), DI-Water (Sigma-Aldrich), (3-Aminoprophyl) trimethoxysilane (APTMS, 97%, Sigma Aldrich), trisodium citrate (Merck), kalium iodide (KI), iodide (I), PEG 4000, chloroform (Merck), acetonitrile, ruthenium N-719 industry standard dye (maroon crystalline powder, Dyesol), CH_3COOH (98%, Brataco) and Triton X-100 (Merck).

Synthesis of Au@TiO_2 Core-shell Photoanodes

AuNP were prepared using Turkevich method [6]. The solution was kept boiling until the color of the solution change to ruby red and a continous stirring was maintained until room temperature was reached [7]. Au@TiO_2 core-shell powder was obtained by mixing the AuNP with Ti^{4+} solution through combination of TTIP (Titanium Isopropoxide) and TEOA (Triethanolamine) in nitrogen atmosphere at molarity ratio of 2:1 (TEOA:TTIP). Volume of Ti^{4+} solution was varied, i.e. 15ml, 20ml, 25ml and 30ml. The washing process of Au@TiO_2 took two weeks using aquades. Subsequently, the powder of Au@TiO_2 photoanodes was calcined for 24 hours at 80^{o}C [8].

Characterization of synthesized Au@TiO_2 core-shell photoanodes

The crystal structure of photoanodes powder was characterized using X-ray diffraction (XRD) (Philips XPert MPD 30 mA, 40 kV) with Cu Kα radiation (λ = 0.15406 nm) with 2θ scanned within the range of 15°-90^o. The particle size distribution of AuNP was carried out using particle size analyzer (PSA) (Malvern Zetasizer). Absorption of photoanode powder in visible light (200 nm-800 nm) was characterized using UV-Vis spectrophotometer Perkin-Elmer Lambda 750 UV/Vis /NIR.

Fabrication of DSSC

Photoanodes powder in the weight of 0.25 grams was made into pasta by dissolution in 87.5 µL in distilled water, 12.5 µL of Triton X-100 and 125 µL of CH_3COOH. Coating of photoanode paste into FTO glass was undertaken by using the doctorblade method. The coated FTO glass was heated at 225^{o}C for 2 minutes using hot plate and then soaked in a ruthenium complex N-719 dye solution for 12 hours. Finally, DSSC components with sandwich structures was made by arranging FTO glass coated with dyed-photoanode, an electrolyte solution, and a platinum-plated FTO glass as a counter electrode. The photocurrent action spectra or IPCE in visible light spectrum was obtained by adjusting wavelength of incident light, i.e. series connection of halogen lamp (GR-150 Halogen Flood Light 150W) and monochromator (CT-10T, JASCO). The value of incident light power was measured by using optical power meter (Thorlab S-120C).

RESULT AND DISCUSSION

XRD Characterizations

Figure 1. shows XRD spectra of Au@TiO_2 samples with various TiO_2 volume. Peak observed 2θ = 25,71°, 24,79°, 25,92°, 25,90° (JCPDS 21-1272) indicated the formation of TiO_2, and peak observed 2θ = 62,99°, 62,95°, 62,93°, 62,98°, (JCPDS 04-0784) indicated the formation of Au (220). However, peak at 2θ = 31.7° in sample with 30ml Ti^{4+} corresponds to NaCl (JCPDS 5-0628). The NaCl formed by the reaction of NaOH with HCl for Au reduction[9,10]. Liao et al [11], have been reported that addition of 1 wt% NaCl solution added into the TiO_2 pastes should increase the

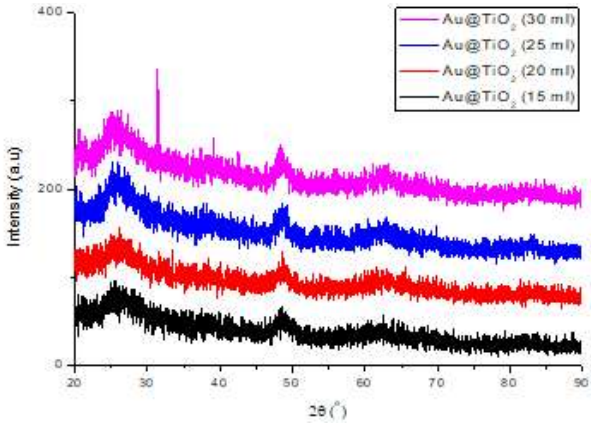

Figure 1. XRD spectra of Au@TiO_2 with various TiO_2 volume.

short-circuit current density and hence efficiency of DSSC increases.

PSA Characterizations

PSA characterization was undertaken for AuNPs only and Au@TiO_2 core-shell. The measurement of AuNP can be done directly because it was in the form of liquid colloid, but for powder-shaped core, dissolution was required with a dose of 5 mg per 10 mL.

The size of cores and shells are tabulated in Table 1. It is seen that the various TiO_2 volume results in the growth of Au@TiO_2. The size distribution of AuNPs only and Au@TiO_2 core-shell shown in Figure 2.

Table 1. Particle size of AuNP and Au@TiO_2

Sample	Avarage Diameter of Core-Shell (nm)
Au	158
Au@TiO_2 (15 mL)	523
Au@TiO_2 (20 mL)	633
Au@TiO_2 (25 mL)	702
Au@TiO_2 (30 mL)	734

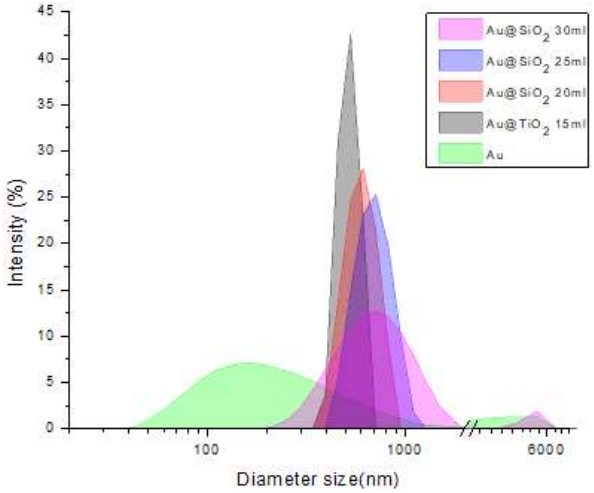

Figure 2. Size distribution of Au@TiO_2 with various TiO_2 volume.

UV-Vis Characterizations

According to UV-Vis characterization (Figure 3), all samples studied show weak surface plasmon resonance response (~520 to 600 nm) as indicative of the thick TiO_2 shells for individual core-shell Au@TiO_2 [11]. All samples reveal a strong peak belongs to TiO_2 at ~320 nm. For TiO_2 effect, only TiO_2 25ml can show the sharpest peak of Au absorbance among other volume variations. As TiO_2 covers the Au surface, an increase in the intensity of the plasmon absorption. An increase in the local refractive index around the nanoparticles has caused the Au peak to shift to a longer wavelength [12]. UV-Vis characterization can also indicate the quality of core-shell structure, whether the shell may or not cover the whole core. Since the absorption produced by the TiO_2 maintains the constant characteristics, this may suggest that the optical properties of TiO_2 shell are not affected by Au cores. The diminution of absorption intensity led by the electronic transition between Au cores and the TiO_2 shells for samples having TiO_2 30 ml may indicate that the interaction between Au cores and

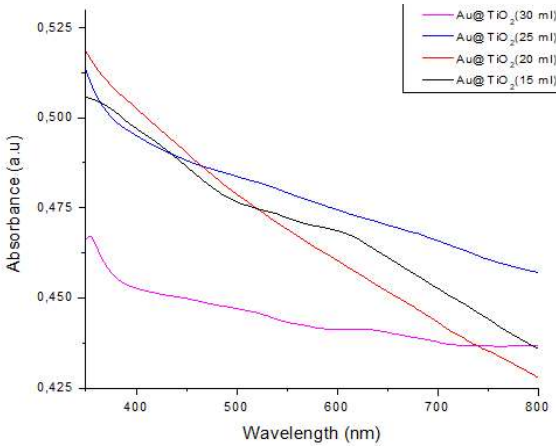

Figure 3. Normalized UV-Vis absorption spectra of the of Au@TiO_2 core-shell nanoparticles synthesized under various TiO_2 volume.

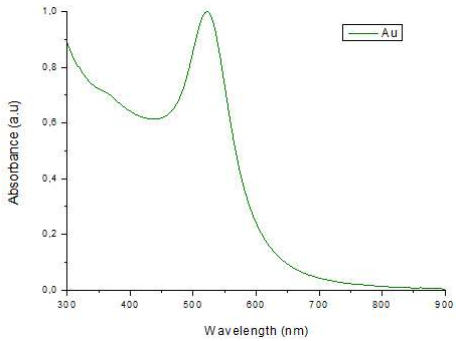

Figure 4. Graph Tauc Plot Core-Shell Au@TiO_2 with various TiO_2 volume.

TiO_2 shells is weakened as the cores are fully covered by the shells. The optical band gap of the Au@TiO_2 core-shell nanoparticles (Table 2) were in the range of 1.7 – 2.4 eV which was substantially lower than that of TiO_2 (~3.20 eV) [13] and was likely attributed to defect-induced narrow band gap [14].

From UV-Vis spectroscopy, the optical band gap from this sample can determined by equation 1-4. The optical band gap of the Au@TiO_2 core-shell nanoparticles (Table 2) were in the range of 1.5 – 2.5 eV which was substantially lower than that of TiO_2.

$$\alpha h\nu^2 = \frac{\alpha hc}{\lambda} \quad \text{.....} \quad (1)$$

$$\alpha = \frac{\ln\frac{100}{T}}{d} \quad \text{.....} \quad (2)$$

$$A = -\log T \quad \text{.....} \quad (3)$$

$$E = h\nu = \frac{hc}{\lambda} \quad \text{.....} \quad (4)$$

Table 2. Electrical band gap of Au@TiO_2

Sample	Optical Band Gap (eV)
Au@TiO_2 (15 mL)	2,0
Au@TiO_2 (20 mL)	1,8
Au@TiO_2 (25 mL)	2,4
Au@TiO_2 (30 mL)	1,6

IPCE Test

Incident photon-to-current conversion efficiency measurement was performed in order to investigate the spectral response of plasmon-enhanced DSSC (Figure 5). In general, the spectra consist of additional peak located at ~450-470 nm. This is attributed to the interaction between Au and TiO_2, and not find in sample without Au. The DSSC using Au@TiO_2 core-shell have incident photon to current conversion higher than that without gold. This is attributed to the effect of LSPR of gold, peak located at 530-600. Our results on incident photon-to-current conversion efficiency indicates that the presence of TiO_2 depending on its volume fraction during synthesis tend to shift to longer wavelength. The thickness of TiO_2 influence the transfer of hot-carriers to TiO_2. Short circuit current density decreases with increasing thickness, as indicative of a fewer hot electrons being transfered to the semiconductor[15].

This can be understood, since part of the photogenerated carriers may be located at the surface of TiO_2 and there will be no injection on it. Thus, this part refers to as loss carriers [16]. Furthermore, the TiO_2 layer must be thin, because bare Au nanoparticles trap electrons and facilitate reduction of I^{3-} to I^- there-by acting as a loss mechanism.

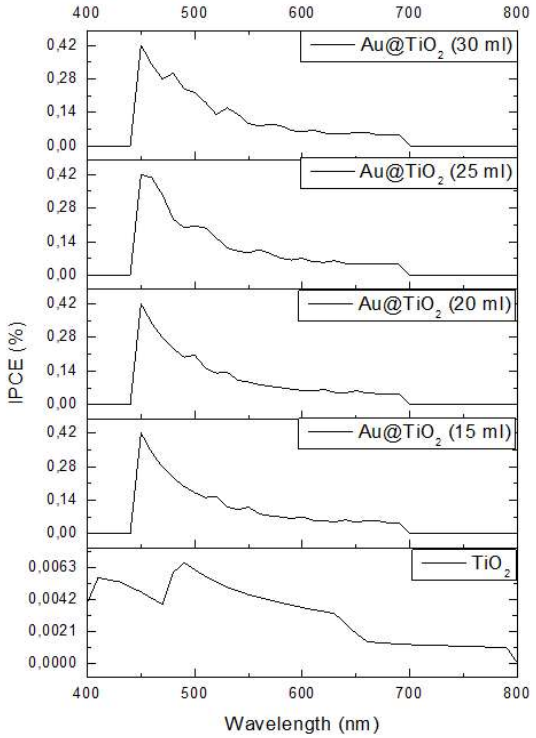

Figure 5. Incident photon to current conversion (IPCE) curves for Core-Shell Au@TiO_2 with various TiO_2.

IV Test

Figure 6 illustrates the J-V curves behavior of studied samples. With the inclusion of Au@TiO_2 core-shell nanoparticles in TiO_2 paste, the cell performance

Table 3. Efficiency of DSSC with various volume of TiO_2

Tipe	Voc (V)	Jsc (mA/cm^2)	Efisiensi (%)
Au@TiO_2 (15 mL)	0,827	0,047	0,023
Au@TiO_2 (20 mL)	0,610	0,056	0,020
Au@TiO_2 (25 mL)	0,876	0,054	0,029
Au@TiO_2 (30 mL)	0,715	0,053	0,024

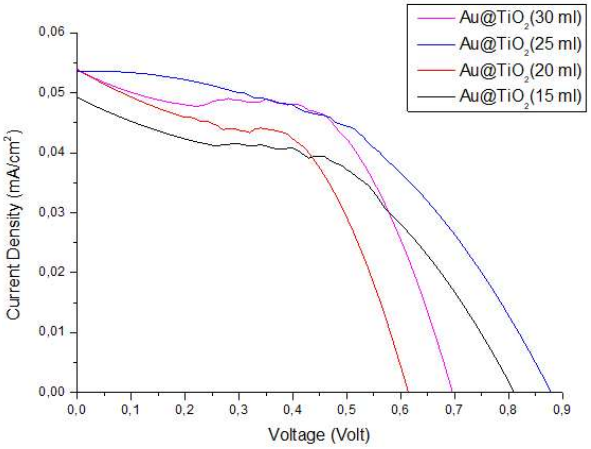

Figure 6. Photocurrent density - voltage curve of the DSSC.

improved substantially. DSSC with Au@TiO_2 having 25 mL volume of TiO_2 shows an improved efficiency. The improved efficiency was largely attributed to the increased J_{SC} and V_{OC}. This enhanced J_{SC} is a result of plasmonic effect of the Au nanoparticles.

CONCLUSION

The addition of Au@TiO_2 core-shell nanoparticles could increase 65.6% incident photon-to-current efficiency (IPCE) compared to that without gold. It shows the typical of LSPR gold. The presence of TiO_2 depending on its volume fraction during synthesis tend to shift to longer wavelength. However, some defects may occur in the system as observed through the reduction in optical energy gap which further may cause decrease in the DSSC performance.

ACKNOWLEDGMENT

This work was funded by the Ministry of Research Technology and Higher Education of Republic of Indonesia.

REFERENCES

[1] W.-L. Liu *et al.*, "The influence of shell thickness of Au@TiO_2 core–shell nanoparticles on the plasmonic enhancement effect in dye-sensitized solar cells," *Nanoscale*, vol. 5, no. 17, p. 7953, 2013.

[2] G. Wan *et al.*, "The Preparation of Au@TiO_2 Yolk–Shell Nanostructure and its Applications for Degradation and Detection of Methylene Blue," *Nanoscale Res. Lett.*, vol. 12, 2017.

[3] J. Qi, X. Dang, P. T. Hammond, and A. M. Belcher, "Highly Efficient Plasmon-Enhanced Dye-Sensitized Solar Cells through," *ACS Nano*, vol. 5, no. 9, pp. 7108–7116, 2011.

[4] C. C. Crane, F. Wang, J. Li, J. Tao, Y. Zhu, and J. Chen, "Synthesis of Copper-Silica Core-Shell Nanostructures with Sharp and Stable Localized Surface Plasmon Resonance," *J. Phys. Chem. C*, vol. 121, no. 10, pp. 5684–5692, 2017.

[5] J. Toudert, R. Serna, and M. Jiménez De Castro, "Exploring the optical potential of nano-bismuth: Tunable surface plasmon resonances in the near ultraviolet-to-near infrared range," *J. Phys. Chem. C*, vol. 116, no. 38, pp. 20530–20539, 2012.

[6] W.-L. Liu *et al.*, "Influence of morphology on the plasmonic enhancement effect of Au@TiO_2 core-shell nanoparticles in dye-sensitized solar cells," *CLEO Sci. Innov.*, pp. 1–21, 2013.

[7] Kwon, H. W., Lim, Y. M., Tripathy, S. K., Kim, B. G., Lee, M. S., & Yu, Y. T. (2007). Synthesis of AU/TiO2 core-shell nanoparticles from titanium isopropoxide and thermal resistance effect of TiO2 shell. *Japanese Journal of Applied Physics, Part 1: Regular Papers and Short Notes and Review Papers*, *46*(4 B), 2567–2570. https://doi.org/10.1143/JJAP.46.2567

[8] C. Nahm *et al.*, "The effects of 100nm-diameter Au nanoparticles on dye-sensitized solar cells The effects of 100 nm-diameter Au nanoparticles on dye-sensitized solar cells," vol. 253107, 2011.

[9] J. Turkevich, G. Garton, and P. C. Stevenson, "THE COLOR OF COLLOIDAL GOLD J. Turkevich, G. Garton, and P. C. Stevenson."

[10] U. Hohenester and A. Trügler, "MNPBEM - A Matlab toolbox for the simulation of plasmonic nanoparticles," *Comput. Phys. Commun.*, vol. 183, no. 2, pp. 370–381, 2012.

[11] J. Waxenegger, A. Trügler, and U. Hohenester, "Plasmonics simulations with the MNPBEM toolbox: Consideration of substrates and layer structures," *Comput. Phys. Commun.*, vol. 193, pp. 138–150, 2015.

[12] X. F. Wu, H. Y. Song, J. M. Yoon, Y. T. Yu, and Y. F. Chen, "Synthesis of core-shell Au@TiO_2 nanopartides with truncated wedge-shaped morphology and their photocatalytic properties," *Langmuir*, vol. 25, no. 11, pp. 6438–6447, 2009.

[13] C. Dette *et al.*, "TiO2anatase with a bandgap in the visible region," *Nano Lett.*, vol. 14, no. 11, pp. 6533–6538, 2014.

[14] S. Kalathil, M. M. Khan, S. A. Ansari, J. Lee, and M. H. Cho, "Band gap narrowing of titanium dioxide (TiO_2) nanocrystals by electrochemically active biofilms and their visible light activity," *Nanoscale*, vol. 5, no. 14, pp. 6323–6326, 2013.

[15] M. M. Khan *et al.*, "Band gap engineered TiO_2 nanoparticles for visible light induced photoelectrochemical and photocatalytic studies," *J. Mater. Chem. A*, vol. 2, no. 3, pp. 637–644, 2014.

[16] H. L. Guo, Q. Zhu, X. L. Wu, Y. F. Jiang, X. Xie, and A. W. Xu, "Oxygen deficient ZnO_{1-x} nanosheets with high visible light photocatalytic activity," *Nanoscale*, vol. 7, no. 16, pp. 7216–7223, 2015.